

1304 – SM2

ENCAPSULATION OF ZIRCONOCENE IN SILICA BY NON-HYDROLYTIC SOL-GEL METHOD

Adriano Fisch¹, Cristiane F. Petry², Dirce Pozebon², Fernanda C. Stedile², Nilo S. M. Cardozo¹, Argimiro R. Secchi¹ e João H. Z. dos Santos²

1-Departamento de Engenharia Química – Universidade Federal do Rio Grande do Sul (UFRGS)

Eng. Luis Englert s/n Campus Central. ZIP: 90040-040 - Porto Alegre - RS – BRAZIL

Phone: (51) 3316-3528 – Fax: (51) 3316-3277 – Email: {fisch, nilo, arge}@enq.ufrgs.br

2- Instituto de Química – Universidade Federal do Rio Grande do Sul (UFRGS)

Av. Bento Gonçalves, 9500 Campus do Vale. ZIP: 91501-970 – Porto Alegre – RS – BRAZIL

Phone: (51) 3316-7238 – Fax: (51) 3316-7304 – Email: jhzds@iq.ufrgs.br

ABSTRACT – Cyclopentadienil zirconium dichloride was encapsulated into a silica matrix prepared by the non-hydrolytic sol-gel method. Three different routes were evaluated in terms of encapsulated zirconocene and catalyst activity in ethylene polymerization, using methylaluminoxane as cocatalyst. Catalysts were characterized by Rutherford backscattering spectrometry, Fourier transform infrared spectroscopy, diffuse reflectance spectroscopy, scanning electron microscopy and X-ray dispersive spectroscopy. The encapsulated Zr content remained between 0.60 and 1.55 wt.% Zr/SiO₂, depending upon the components ratio and Lewis acid catalyst employed in the sol-gel synthesis. Catalyst grains were of irregular shape (20 – 100 μm) and zirconocene distribution was not uniform. All the systems were shown to be active in ethylene polymerization. Catalyst activity was intermediate between that exhibited by the homogeneous and the grafted zirconocene on silica. Resulting polyethylenes presented narrow molecular weight distribution and molecular weight slightly higher than that observed in the case of polymer produced with the homogeneous system.

KEYWORDS: supported metallocene, sol-gel, encapsulation, polyethylene

1. INTRODUCTION

Metallocene catalysts can polymerize α -olefins with high activity and excellent stereochemistry control. The key of the success of these catalysts is that in such highly active systems the control of the coordination sphere around the metal center allows to define the polymer properties (Kaminsky, 1999; and Hlatky, 2000a, for instance). Nevertheless, their industrial application in the current plants, which are designed to run heterogeneous Ziegler-Natta catalysts, is only possible if such systems are supported on suitable carriers.

In order to generate heterogeneous metallocene systems, several methods have been proposed in the literature (Hlatky, 2000b). Silica has been largely the most employed support (dos Santos *et al.*, 1997, 1999 e 2001). Nevertheless, other supports have been investigated, including for example mobile crystalline materials (MCM), SBA-15, and zeolites, as well as organic supports such as polymers (Liu *et al.* 2004; Dong *et al.*, 2005; Marques and Moreira, 2003; Ko and Woo, 2003; and Wu *et al.*, 2005). Chemical modifiers such as MAO (Liu *et al.*, 2004), TMA (Costa *et al.*, 2005) and organosilanes (Alonso *et al.*, 2004) have been proposed to generate more stable and spaced surface species, avoiding bimolecular deactivation reactions. However, despite the va-

riety of the approaches proposed on the literature for the immobilization of zirconocenes, for the knowledge of the authors, the encapsulation of zirconocenes into SiO_2 has not already been reported.

Encapsulation consists of trapping the catalyst within oxide or polymer network. This methodology has been investigated for immobilization of biomolecules, such as enzymes, metalloproteins, photoactive biomolecules, protozoa cell, and of precursor salts of metallic oxides and catalytic complexes (Livage, 1997; Dunn *et al.*, 1998; Kato *et al.*, 2002; and Drechsel *et al.*, 2004). The main characteristic of this method is preserving the properties of the substance or organism trapped within the oxide network. These processes allow to obtain solid materials by gelation, where an oxide network is created by progressive polycondensation reactions of molecular precursors in liquid medium, rather than by crystallization or precipitation. Nevertheless, such method usually involves the use of aqueous (acid or basic) solution, which per se is not possible due to the lability of zirconocenes. The non-hydrolytic sol-gel approach is a potential route to zirconocene encapsulation, since it avoids the use of water (Hay and Haval, 1998).

In the present work, the encapsulation of Cp_2ZrCl_2 within the silica network using a non-hydrolytic sol-gel process is reported. The resulting supported systems were characterized by spectroscopic techniques and evaluated in ethylene polymerization, using MAO as cocatalyst.

2. MATERIALS AND METHODS

2.1 Chemicals and Reagents

All the employed chemicals were analytical reagent grade and all experiments were performed under inert atmosphere (argon) using

the Schlenk technique. Silicon tetrachloride (Merck), titanium tetrachloride (Merck), tetraethylorthosilicate (TEOS, Merck), triethylaluminum toluene solution (TEA; Akzo Nobel) and cyclopentadienyl zirconium dichloride (Cp_2ZrCl_2 ; Aldrich) were used as received. Toluene and n-hexane were purified by distillation on metallic sodium and benzofenone. Iron(III) chloride (95%; Merck) was dried by vacuum at room temperature for 2h. Silica Grace 948 ($255 \text{ m}^2 \cdot \text{g}^{-1}$) was activated under vacuum ($P < 10^{-4}$ mbar) for 16 h at 450°C . The support was then cooled to room temperature under vacuum and stored under dried Argon.

2.2 Metallocene Encapsulation

Three encapsulation routes, based on non-hydrolytic method (Hay and Haval, 1998; and Bourget *et al.*, 1998), were evaluated in the synthesis of supported catalysts. The method consists in reacting SiCl_4 and $\text{Si}(\text{OC}_2\text{H}_5)_4$ using a Lewis acid as catalyst. Previous studies were accomplished in order to evaluate the effect of other Lewis acids (e.g. AlCl_3), temperature, reactant addition order, and $\text{SiCl}_4:\text{Si}(\text{OC}_2\text{H}_5)_4$ ratio on the encapsulation. Syntheses accomplished in this work were based on the results obtained from these previous studies.

In the present case, the sol-gel reaction occurs in presence of Cp_2ZrCl_2 , having FeCl_3 or TiCl_4 as catalyst. Figure 1 shows the general procedure used for the zirconocene encapsulation using the molar ratios reported on Table 1. Based on the results of the previous studies, different molar ratios [$\text{SiCl}_4:\text{Si}(\text{OC}_2\text{H}_5)_4$], were employed: 2:1 (A); 1:1 (B) and 1:2 (C). In the routes A and B, FeCl_3 was used as Lewis acid catalyst while in C, TiCl_4 . In a typical experiment, Cp_2ZrCl_2 was dissolved in toluene (1 cm^3), followed by the addition of the Lewis acid (TiCl_4 or FeCl_3) and the oxygen donor (TEOS). All experiments were performed at $70(\pm 2)^\circ\text{C}$. After the gelation time has been reached, the resulting oxide was washed

(ca. 20cm³) with a TEA n-hexane solution (ca. 0.5wt.%) at room temperature in order to eliminate residual ethoxide groups (dos Santos *et al.*, 2001). Further, the solid was then dried by vacuum for 12 h at room temperature. For comparison, the corresponding grafted zirconocene was synthesized according to the protocol described in the literature (dos Santos *et al.*, 1997).

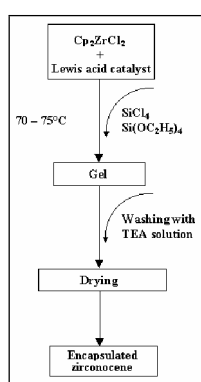


Figure 1 - General procedure for encapsulation.

Table 1 - Molar ratios evaluated in the 3 synthetic routes.

Route	SiCl ₄ :Si(OC ₂ H ₅) ₄ (molar ratio)	Lewis acid catalyst (wt.%)
A	2:1	0.25 (FeCl ₃)
B	1:1	0.25 (FeCl ₃)
C	1:2	32.0 (TiCl ₄ *)

*molar ratio SiCl₄:TiCl₄:Si(OC₂H₅)₄ 1:1:2

2.3 Catalyst Characterization

Rutherford Backscattering Spectrometry (RBS): Zr loadings in catalysts were determined by Rutherford Backscattering Spectrometry (RBS) using He⁺ beam of 2.0 MeV incident on homogeneous tablets of the compressed (12 MPa) powder of the catalyst systems. For an introduction to the method and applications of this technique the reader is referred elsewhere (Stedile and dos Santos, 1998).

Inductively coupled plasma optical emission spectroscopy (ICP-OES): an inductively coupled plasma optical emission spec-

troscopy from Perkin Elmer (Optima[®] 2000 DV) was used for the measurement of Zr in the catalyst leaching tests.

Fourier-Transformed Infrared Spectroscopy (FT-IR): Infrared Spectroscopy measurements were carried out in a Shimadzu FTIR 8300 spectrophotometer coadding 32 scans at 4 cm⁻¹ resolution. Samples were analyzed as self-supported pellets, using KBr, in transmission mode. FTIR was used for identification of silica matrix and zirconocene. Table 2 shows the bands assigned to silica.

Table 2 - Main assignments of the FTIR.

Assignments	cm ⁻¹
Si-O-C ₂ H ₅ (stretching)	1174
C-C (stretching)	1155
Si-O-Si, infinite chain (stretching)	1090
Si-O (angular deformation)	964
Si-O-Ti (stretching)	918
O-H, single (stretching)	850
C-H (out-of-plane deformation)	830-701
OH, geminal (stretching)	800

Ultraviolet - DRS Spectroscopy (UV-DRS): Diffusion Reflectance in the UV-vis region was measured in a Varian Cary 100. Samples were prepared as self-supported pellets.

X-Ray Diffraction (XRD): the XRD analyses were performed in a Rigaku (DMAX 2200) diffractometer equipped with a Cu tube and secondary monochromator, theta-theta Ultima goniometer and scintillation (NaI (TI)) detector. Samples were analyzed as powder at room temperature.

Scanning Electron Microscopy and X-Ray Energy-Dispersive Spectroscopy: Scanning Electron Microscopy (SEM) and X-Ray Energy Dispersive (EDX) were performed in a JSM 5800 (JEOL) microscope, operating between 10 and 20 kV.

Nitrogen sorption studies: a Micromeritics Gemini was used for nitrogen sorption

studies. The specific surface area was determined by the Brunauer-Emmett-Teller (BET) method at $-196\text{ }^{\circ}\text{C}$, in the partial pressure range of $0.01 < P/P_0 < 0.25$ and, the total pore volume was obtained from the N_2 desorption isotherm.

2.4 Catalyst Evaluation

Polymerization reactions: ethylene polymerization reactions were performed in 150cm^3 of toluene in a 300cm^3 Pyrex glass reactor at constant temperature. MAO was used as cocatalyst in the Al/Zr range from 1000 to 2000. For each experiment, a mass of catalyst system corresponding to 10^{-5}M of the metal was suspended in 5cm^3 of toluene and transferred into the reactor under argon. The polymerizations were performed with 1.6bar of absolute pressure of ethylene at 60°C for 30min. Acidified (HCl) ethanol was used to quench the processes, and reaction products were separated by filtration, washed with distilled water, and finally dried under reduced pressure at 60°C . The homogenous polymerizations were carried out in the same way.

Catalyst leaching: this test was performed using a mass of catalyst corresponding to 10^{-6}mol of Zr which was suspended into 150cm^3 of toluene in the presence of MAO (Al/Zr = 2000). The system was stirred for 1h at 60°C and then filtered through a fritted disk. The filtered solution was transferred into the reactor under argon. The polymerization reactions were carried out according previous description. ICP-OES was used for determining the Zr content in the eluated.

Polymer characterization: polymers were characterized by melting point and crystallinity using a Perkin-Elmer DSC 4 differential scanning calorimeter. Molar masses and molar mass distributions were investigated with a Waters 150C high-temperature GPC instru-

ment at 140°C , equipped with refraction index detector and three columns (Styragel[®] HT 3, HT 5 e Ht 6E toluene). TCB was used as solvent at a flow rate of $1\text{cm}^3\cdot\text{min}^{-1}$.

3. RESULTS AND DISCUSSION

3.1 Catalyst Synthesis and Characterization

In table 3 is shown the resulting encapsulated Zr content within the catalyst.

Table 3 - Cp_2ZrCl_2 encapsulated into oxide matrices.

Route	Encapsulated zirconocene
A	0.60 wt.% Zr/SiO ₂
B	1.02 wt.% Zr/SiO ₂
C	1.55 wt.% Zr/(SiO ₂ -TiO ₂)

In the route A, it was used the ratio 2:1 of the $\text{SiCl}_4:\text{Si}(\text{OC}_2\text{H}_5)_4$. In the routes B and C, the stoichiometric ratio $\text{SiCl}_4:\text{Si}(\text{OC}_2\text{H}_5)_4$ and $\text{SiCl}_4:\text{TiCl}_4:\text{Si}(\text{OC}_2\text{H}_5)_4$ was employed, respectively. When excess of SiCl_4 was used (A), all the $\text{Si}(\text{OC}_2\text{H}_5)_4$ might be reacted and the generated mass of oxide matrix is higher than in the stoichiometric route (B and C) probably due to equilibrium displacement. Therefore, the routes B and C have exhibited higher contents of the zirconium in the catalyst that could be attributed to lower conversion of the reactants to oxide matrix. According to Table 3, the encapsulated zirconocene content is related to the $\text{SiCl}_4:\text{Si}(\text{OC}_2\text{H}_5)_4$ ratio.

The catalysts were further characterized by complementary techniques. Figure 2 shows a typical IR spectrum of the encapsulated catalysts. Most of the assigned bands refer to the oxide matrix (Vansant et al., 1995; Colthup, 1990; and Nakamoto, 1997). The presence of silica can be observed by the strong band centered at 1090cm^{-1} , attributed to the Si-O-Si stretching, which was present in the three catalysts (Figure 2).

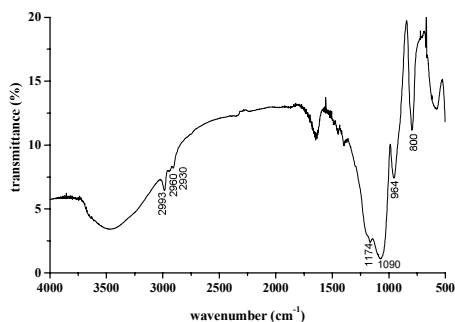


Figure 2 - IR spectrum for encapsulated zirconocene obtained by route B.

The band presented at 1174cm^{-1} can be assigned to Si-O-C stretching, probably due to residual ethoxide groups, confirmed also by the presence of C-H stretching at $2800\text{-}2950\text{cm}^{-1}$ region. Besides, surface species resulting from the washing with TEA might also have generated Si-O-C species. It is worth noting that a band at 918cm^{-1} was observed in the case of catalyst obtained by route C. This band can be attributed to Si-O-Ti stretching, suggesting that Ti moieties (from the TiCl_4 employed as catalyst) might be incorporated to the network. The C-C stretching and C-H out-of-plane deformation of cyclopentadienyl rings might be overlaid by Si-O-Si and OH (geminal) on the all spectra. Therefore, the presence of the zirconocene into silica could not be determined by FTIR measurement.

The catalysts were further analyzed by UV-DRS in order to try to detect the presence of the zirconocene species. According to Figure 3, two bands are observed in the case of Cp_2ZrCl_2 , at 320 and 370nm, which could be assigned to ligand metal charge transfers (LMCT) $\text{Cl}\rightarrow\text{Zr}$ and $\text{Cp}\rightarrow\text{Zr}$, respectively (Nakamoto, 1997; and Costa, 2005). These bands, as expected, were found in zirconoceno spectrum. The band attributed to LMCT $\text{Cp}\rightarrow\text{Zr}$ was also observed in the case of routes A and B. The transition LMCT $\text{Cl}\rightarrow\text{Zr}$ is less clear and might be reduced due to Cl reaction during

the oxide matrix synthesis or during the washing step with TEA. It is clear that the electronic spectrum of the resulting catalyst obtained by route C is different; suggesting that the presence of Ti in the network might influence somehow the resulting encapsulated species. In this way, it seems that the coordination sphere of the zirconium did not undergo modification by the heterogeneous route.

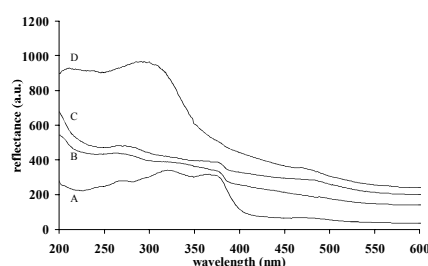


Figure 3 - UV-DRS spectrum: (A) Cp_2ZrCl_2 pure, (B) route A, (C) route B, and (D) route C.

The morphology of the catalysts was given by SEM images. Figure 4 shows the catalyst grain obtained for the route C which has irregular form and sizes in the range of $20\text{-}100\mu\text{m}$. Similar micrographies were observed for the catalyst obtained by the two other routes.

The catalysts were further analyzed by SEM-EDX. Figure 5 shows the microanalysis of the encapsulated catalyst obtained by route C. Elemental analysis distribution shows the presence of Zr, Cl, Si, Ti and Al, suggesting the presence of residual Ti (from the Lewis acid catalyst), which might have been incorporated to the network as observed by FT-IR analysis. Cl is assigned to the Cp_2ZrCl_2 , as well as to residual SiCl_x and TiCl_x . Besides, according to EDX measurements at different spots of the catalyst sample, the Zr distribution is not homogeneous along the grain.

Catalyst analysis by XRD, as expected, has shown that the oxide matrix was amorphous for all the systems, presenting two halos centered at 17 and 220.

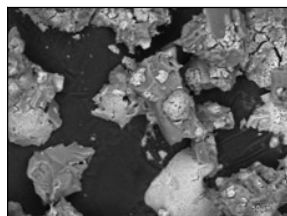


Figure 4 - SEM micrographics for catalyst obtained by route C.

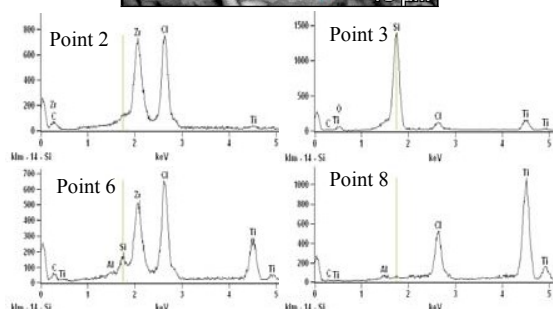
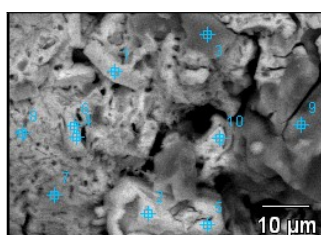


Figure 5 - Elemental distribution in catalyst C, measured by SEM-EDX.

The determination of the porosity or pore radii of the samples by nitrogen sorption demonstrated that all encapsulated catalyst have low surface area, ca. $10\text{m}^2/\text{g}$, probably due to pore collapse during the drying process.

3.2 Catalyst Evaluation

The encapsulated zirconocene were evaluated in ethylene polymerization having MAO as cocatalyst (Table 4). For comparison, data from the homogeneous catalyst and from that grafted on silica were also included. Encapsulated Cp_2ZrCl_2 obtained by route A loses activity as Al/Zr decreases. This difference might also be accounted for encapsulated Zr content, being catalyst A the one with the lowest metal loading, and therefore, more prone to poisoning.

As shown in Table 4, all the encapsulated zirconocenes were active in ethylene polymerization. The highest activity was observed for the catalyst obtained by route B. Nevertheless, the most stable and active in the 2000-1000 Al/Zr range was that obtained by route C. It is worth noting that the supported catalyst obtained by grafting on silica presented lower activity than the other systems. In comparison to the homogeneous system, such behavior is expected since the silica surface plays the role of huge ligand hindering the access to the monomer. The encapsulated system presents intermediate catalyst activity, suggesting that the homogeneous nature of the zirconocene might have been preserved. Nevertheless, in this case, the access of the monomer to catalyst centers is also hampered, which is probably responsible for the reduction in catalyst activity in comparison to the homogeneous one. Comparing the encapsulated to the grafted system, the former as already mentioned, presents higher catalyst activity. In addition to the steric effect played by the support itself, it is believed that only roughly ca. 1.0% of the total grafted species is indeed active (Muñoz-Escalona, 1998). Thus, since in the encapsulated process, no reaction between silanol groups and zirconocene ligands are involved (as in the case of grafting) this process is not responsible for the lower activity. In this case, the monomer access to zirconocene molecules inside the silica support might be the major limiting factor influencing catalyst activity. Especially since very low specific surface areas were determined by the BET method, suggesting the presence of a silica matrix with very low porosity.

The stability of the encapsulated catalyst in terms of leaching from MAO cocatalyst was evaluated by measuring the Zr in the eluted fraction through ICP-OES. The Zr content was shown to be $10\ \mu\text{g}\cdot\text{L}^{-1}$ for all encapsulated catalysts. Therefore, leaching process during polymerization was considered very unlikely.

Table 4 - Catalyst activity and polymer characteristics.

Catalyst	Al/Zr	Activity ($\text{k}_{\text{pol}} \cdot \text{mol}_{\text{Zr}}^{-1}$)	T_m ($^{\circ}\text{C}$)	χ (%)	M_w ($\text{kg} \cdot \text{mol}^{-1}$)	M_w/M_n
A (0.60 wt.% Zr/SiO ₂)	2000	1400	133	51	230	2.0
	1500	135	132	56	130	3.2
	1000	traces	-	-	-	-
B (1.02 wt.% Zr/SiO ₂)	2000	1900	135	70	153	2.1
	1500	220	134	51	133	2.6
	1000	80	133	46	130	2.5
C (1.55 wt.% Zr/(SiO ₂ +TiO ₂))	2000	1800	133	65	124	2.5
	1500	1330	133	59	198	3.2
	1000	1230	134	44	196	2.4
Cp ₂ ZrCl ₂ homogeneous	2000	3000	133	-	100	2.2
	1500	2750	133	66	120	2.3
Cp ₂ ZrCl ₂ /SiO ₂ (0.4 wt.% Zr/SiO ₂)	2000	1300	136	-	90	2.8

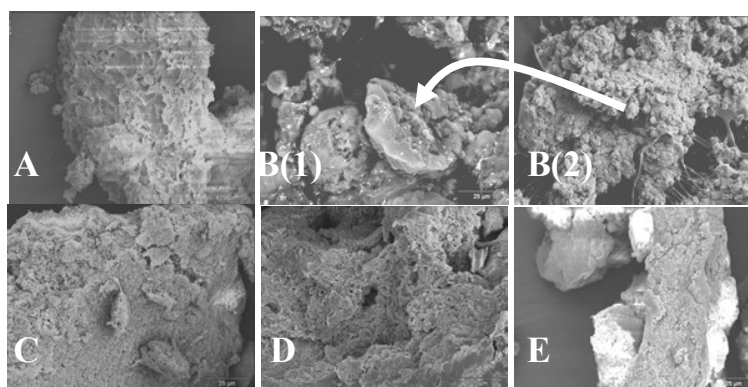


Figure 6 - SEM micrographics for nascent polymer obtained by encapsulated catalysts. Homogeneous polymerization of zirconocene (A, magnification 1000x), supported zirconocene on silica 948 (B(1) and B(2), magnification 1000x and 100x, respectively), encapsulated route A (C, magnification 1000x), encapsulated route B (D, magnification 1000x) and encapsulated route C (E, magnification 1000x).

3.3 Polymer Characterization

The resulting polyethylenes were characterized by DSC and GPC (Table 4). The values obtained for melting temperature (T_m) and the degree of crystallinity (χ) are near those obtained by homogeneous catalyst. Besides, it is curious that the M_w observed for the polymers obtained with the encapsulated zirconocenes is slightly higher than that produced with the homogeneous. It seems that the silica matrix might impinge some effect during the polymerization process hindering, for instance,

termination reactions or affording a higher stability of the catalyst center during polymer chain growing steps. Further studies are necessary to elucidate such possibilities and the effects on the kinetic mechanism mainly on the propagation and termination reactions.

Morphology of the nascent polymers (polymers obtained in the early stages of the polymerization) was evaluated through SEM (Figure 6). It could be noted that the polymer obtained with encapsulated zirconocene has more similar particle morphology with respect to ho-

mogeneous catalyst than with the supported on commercial silica.

4. FINAL REMARKS

Zirconocene encapsulation into a silica matrix, synthesized by non-hydrolytic sol-gel method was shown to be a potential strategy for developing heterogeneous metallocene catalysts. This preliminary study showed that the ratio of the matrix components influences on the encapsulated Zr content as well as on the catalyst activity in ethylene polymerization. In spite of the fact that the nature of the catalyst species might be closer to the homogeneous ones, the environment might somehow influence the polymerization process, since polyethylenes with higher molecular weight were obtained. The heterogeneous distribution of Zr in the grain and the very low catalyst specific surface area are drawbacks, which have to be overcome. Nevertheless this heterogenisation route seems to allow to avoid some inconvenient usually observed in the case of zirconocene grafting, such as catalyst leaching or very low grafted content, which, in turn, depends on the availability of surface silanol groups and on the steric effect played by the coordination sphere of the metallocenes.

4. REFERENCES

- KAMINSKY, W. Metalorganic catalysts for synthesis and polymerization: recent results by Ziegler-Natta and metallocene investigations, Springer-Verlag: Berlin, 1999;
- HLATKY, G.G. In: Metallocene-based polyolefins, J. Scheirs, W. Kaminsky (Eds). John Wiley: West Sussex, 2000;
- HLATKY, G.G. Chem. Rev. 100 (2000) 1347;
- LIU, C., TANG, T. and HUANG, B. J. Catal. 221 (2004) 162;
- DONG, X.; WANG, L.; JIAN, G.; ZHAO, Z.; SUN, T.; YU, H. and WANG, W. J. Mol. Catal. A: Chemical 240 (2005) 239;
- MARQUES, M.F.V. and MOREIRA, S. C., J. Mol. Catal. A: Chemical 192 (2003) 93;
- KO, Y.S. and WOO, S.I. Eur. Polym. J. 39 (2003) 1553;
- WU, L.; ZHOU, J.-M.; LYNCH, D.T. and WANKE, S.E. Appl. Catal. 293 (2005) 180;
- DOS SANTOS, J.H.Z.; DORNELES, S.; STEDILE, F.C.; DUPONT, J.; FORTE, M.C. and BAUMVOL, I.J.R. Macromol. Chem. Phys. 198 (1997) 3529;
- DOS SANTOS, J.H.Z.; KRUG, C.; DA ROSA, M.B.; STEDILE, F.C.; DUPONT, J. and FORTE, M.C. J. Mol. Catal. A: 139 (1999) 199;
- ALONSO, C.; ANTIÑOLO, A.; CARRILLO-HERMOSILLA, F.; CARRIÓN, P.; OTERO, A.; SANCHO, J. and VILLASEÑOR, E.J. Mol. Catal. A: Chem. 220 (2004) 285;
- DOS SANTOS, J.H.Z.; BAN, H.T.; TERANISHI, T.; UOZUMI, T.; SANO, T. and SOGA, T. Appl. Catal. A: General 220 (2001) 287;
- LIVAGE, J. Curr. Opin. Solid State Mater. Sci. 2 (1997) 132;
- DUNN, B.; MILLAR, J.M.; DAVE, B.C.; VALENTINE, J.S. and ZINK, J.I. Acta Mater. 46 (1998) 737;
- KATO, K.; GONG, Y.; SAITO, T. and YOKOGAWA, Y. Biosci. Biotechnol. Biochem. 66 (2002) 221;
- DRECHSEL, S.M.; KAMISKI, R.C.K.; NAKAGAKI, S. and WYPYCH, F.J. Colloid Interface Sci. 277 (2004) 138;
- HAY, J.N. and RAVAL, H.M.J. Sol-Gel Sci. Technol. 13 (1998) 109;
- BOURGET, L.; CORRIU, R.J.P.; LECLEREQ, D.; MUTIN, P.H. and VIOUX, A. J. Non-Cryst. Solids 242 (1998) 81;
- STEDILE, F.C. and DOS SANTOS, J.H.Z. Nucl. Inst. Meth. Phys. Res. B, 136-138 (1998) 1259;
- VANSANT, E.F.; VAN DER VOORT, P. and VRANCKEN, K.C. *Characterization and chemical modification of the silica surface*. Elsevier, Amsterdam, 1995;
- COLTHUP, N. B. Introduction to Infrared and Raman Spectroscopy, 3rd Ed., San Diego: Academic, c1990;
- NAKAMOTO, K. Infrared and Raman Spectra of Inorganic and Coordination Compounds, 5th Ed., New York: John Wiley, 1997;
- COSTA, F.G.; BRAGA, E.A.; BRANDÃO, S.T.; ESPELETA, A.F.; DA ROCHA, Z.N.; SIMPLÍCIO, L.M.T. AND SALES, E.A. Appl. Catal. A: Gen. 290 (2005) 221;
- MUNÓZ-ESCALONA, A.; HIDALGO, G.; LAFUENTE, P.; MARTINEZ-NUÑEZ, M.F.; MÉNDEZ, L.; MICHIELS, W.; PEÑA, B. and SANCHO, J. "Proceeding of 5th International Congress on Metallocene Polymers", 1998, Düsseldorf, Germany, p. 73.